

Optical Absorption by Small Polarons in *p*- and *n*-Type Lanthanum Cobaltite

R. MÜHLSTROH

Philips Research Laboratories, Aachen, Germany

AND

H. G. REIK

Physikalisches Institut der Universität, Freiburg, Germany

(Received 26 May 1967)

Experimental data for the absorption coefficient of *p*- and *n*-type LaCoO₃ are presented for wavelengths between 3 and 14 μ for the temperatures $T_1=290^\circ\text{K}$, $T_2=200^\circ\text{K}$, $T_3=77^\circ\text{K}$, $T_4=4.2^\circ\text{K}$, and four different dopant concentrations. At high temperatures, the absorption coefficient has a minimum at 11 μ . The frequency dependence and the absolute magnitude of the optical absorption cannot be explained by a Drude-Zener-type carrier absorption. At $T_4=4.2^\circ\text{K}$ considerable structure is seen in the absorption. This structure cannot be ascribed to localized modes due to the dopant atoms. The data at T_2 and T_3 show the gradual change of the absorption from high- to low-temperature behavior. The data at T_1 and T_4 can be consistently explained using the high- and low-temperature versions of the small-polaron theory. The agreement between theory and experiment is quantitative for T_1 and for T_4 in the region between 3 and 8 μ . For higher wavelengths the agreement is only qualitative because of the incomplete knowledge of the lattice properties which is needed in order to explain the two-phonon structures in the polaron absorption.

I. INTRODUCTION

IN two recent papers^{1,2} expressions for the frequency dependence of the optical absorption due to small polarons have been presented for the cases of high and low temperature. The underlying physical picture and the results of the theory can be summarized as follows.

The polaron transitions are accompanied by the emission and absorption of optical phonons. For all light frequencies ω one gets contributions to the optical absorption by all possible energy-conserving processes. Consider a particular light frequency and a particular energy-conserving process. Characterize this process by the total number ζ of phonons involved, that is, by the sum of the number of phonons emitted and the number of phonons absorbed. Furthermore, characterize the electron-phonon interaction by the average number η of optical phonons (average frequency $\bar{\omega}$) that contribute to the buildup of the polarization around a localized polaron. (In contradistinction to ζ , the number η is not necessarily an integer.)

Let us now consider the high-temperature case. Here the theory says that for all light frequencies the main contribution to the optical absorption is from processes with values of ζ close to η . This means that for $\omega < \eta\bar{\omega}$, the difference processes with $\zeta \approx \eta$ will contribute more than the sum processes with $\zeta < \eta$, which are less likely to occur. For $\omega \approx \eta\bar{\omega}$, the main contribution is from sum processes in which η phonons are emitted and no phonon is absorbed. For $\omega > \eta\bar{\omega}$, energy-conserving processes are only possible for $\zeta > \eta$. Because these are increasingly less likely to occur, the optical absorption will decrease if the light frequency is further increased. This is plausible because the light cannot do better

than totally strip the polarization of the polaron in a hopping process.

Let us now turn to low temperatures. For high frequencies $\omega \geq \eta\bar{\omega}$, where even at high temperatures the contribution of the sum processes prevails, and the optical absorption is independent of the temperature. At frequencies $\omega < \eta\bar{\omega}$, however, the difference processes with $\zeta \approx \eta$ die out and only the sum processes $\zeta < \eta$ survive. In this frequency range the absorption is decreased with decreasing temperature. Furthermore, phonon structures will make their appearance in the absorption, which, for a sufficiently small spread in the electronic energy, are completely determined by the phonon-dispersion laws.

In this paper we present measurements of the optical absorption in *p*- and *n*-type lanthanum cobaltite for wavelengths between 3 and 14 μ for the temperatures $T_1=290^\circ\text{K}$, $T_2=200^\circ\text{K}$, $T_3=77^\circ\text{K}$, $T_4=4.2^\circ\text{K}$, and four different dopant concentrations. It is shown that the results of the small-polaron theory for high and low temperatures allow for a consistent interpretation of the optical data taken at T_1 and T_4 for one common set of parameters of the theory. The data taken at T_2 and T_3 show the gradual change in the character of the optical absorption and in particular the appearance of phonon structures with decreasing temperature.

For the presentation of our results we proceed as follows: The results of the small-polaron theory for high and low temperatures are summarized without derivation in Sec. II. In Sec. III a short description of the experimental techniques is given. In Sec. IV the optical data are presented and discussed. Their analysis in terms of the small-polaron theory is carried out in Sec. V.

¹ H. G. Reik and D. Heese, *J. Phys. Chem. Solids* **28**, 581 (1967).

² H. G. Reik, *Z. Physik* **203**, 346 (1967).

II. SUMMARY OF SMALL-POLARON-THEORY RESULTS

In the frequency range under study, the absorption coefficient $K(\omega, T)$ is the sum of two contributions, the carrier contribution and the lattice contribution.

$$K(\omega, T) = K_{\text{carr}}(\omega, T) + K_{\text{latt}}(\omega, T). \quad (1)$$

In the range of small dopant concentrations the carrier contribution is directly related to the real part of the electrical conductivity:

$$K_{\text{carr}}(\omega, T) = \text{Re}\sigma(\omega, T) / n\epsilon_0 c. \quad (2)$$

Here ϵ_0 is the dielectric constant of the vacuum ($\epsilon_0 = 8.86 \times 10^{-14}$ A sec/V cm) and n is the index of refraction. The theoretical expressions for the real part of the electrical conductivity will now be summarized.³

A. The High-Temperature Case

In this case $\text{Re}\sigma(\omega, \beta)$ with $\beta = 1/kT$ is given by the following equations:

$$\text{Re}\sigma(\omega, \beta) = \sigma(\omega = 0, \beta) \times \frac{\sinh(\frac{1}{2}\hbar\omega\beta) \exp[-\omega^2\tau^2r(\omega)]}{\frac{1}{2}\hbar\omega\beta [1 + (\omega\tau\Delta)^2]^{1/4}}, \quad (3)$$

$$\sigma(\omega = 0, \beta) = Ne\mu(\omega = 0, \beta), \quad (4)$$

$$\mu(\omega = 0, \beta) = 2J^2 a^2 e^2 \beta \tau \pi^{1/2} \hbar^{-2} \exp[-\eta \tanh(\frac{1}{4}\hbar\bar{\omega}\beta)], \quad (5)$$

$$r(\omega) = (2/\omega\tau\Delta) \ln\{\omega\tau\Delta + [1 + (\omega\tau\Delta)^2]^{1/2}\} - [2/(\omega\tau\Delta^2)] \{[1 + (\omega\tau\Delta)^2]^{1/2} - 1\}, \quad (6)$$

$$\Delta = 2\bar{\omega}\tau, \quad (7)$$

$$\tau^2 = [\sinh(\frac{1}{2}\hbar\bar{\omega}\beta)] / 2\bar{\omega}^2 \eta. \quad (8)$$

Here N is the dopant concentration and a is the lattice constant. From a theoretical point of view, the system of Eqs. (3)–(8) contains three parameters to be determined: the bare electronic resonance integral J , the average frequency of the optical phonons $\bar{\omega}$, and the number η , characterizing the strength of the electron-phonon interaction. The other parameters Δ and τ are determined by (7) and (8). The system (3)–(8) is applicable, provided that the electronic resonance energy J (which is proportional to the bare bandwidth) is smaller than the electron-phonon interaction:

$$J < \eta\hbar\bar{\omega}. \quad (9)$$

From the practical point of view there is only one important parameter, η , free for a fit. The average frequency $\bar{\omega}$ corresponds to a wavelength in the high-frequency reststrahlen band of the substance under study. The possible values of $\bar{\omega}$ are therefore rather restricted, as shown by Fig. 1. Furthermore, in Eq.

³ This refers to only the nondiagonal contributions to $\text{Re}\sigma(\omega, T)$, which, in LaCoO_3 , are the only important ones given. For the general case, where nondiagonal and diagonal contributions are important, see Ref. 2, Sec. 3.

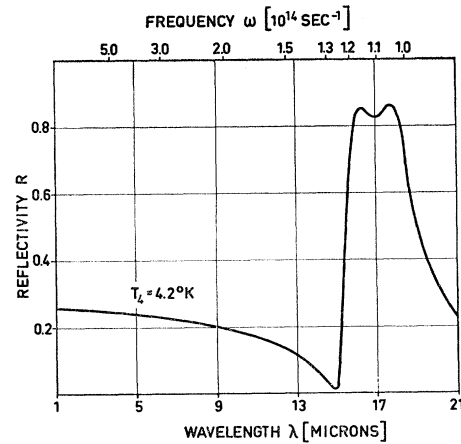


FIG. 1. Reflectivity of LaCoO_3 , $T_4 = 4.2^\circ\text{K}$.

(3), the measured dc conductivity can be taken because of the fact that in LaCoO_3 no diagonal (banding) contributions are present.

B. The Case of Low Temperatures ($\beta \rightarrow \infty$) and High Frequencies ($\omega > 2\bar{\omega}$)

In this case, $\text{Re}\sigma(\omega, \beta \rightarrow \infty)$ is given by the following equation:

$$\text{Re}\sigma(\omega, \beta \rightarrow \infty) = \sqrt{2} J^2 a^2 e^2 N \pi^{1/2} \hbar^{-3} \bar{\omega}^2 e^{-\eta} \times (\bar{\omega}/\omega)^{(\omega/\bar{\omega} + 3/2)} \eta^{\omega/\bar{\omega}} \exp(\omega/\bar{\omega}). \quad (10)$$

This equation contains the same parameters as before. Suppose that a successful fit of the high-temperature optical absorption has been carried out, using the experimental values of the dc conductivity. From this fit the values of η and $\bar{\omega}$ are known. The frequency dependence of the low-temperature formula (10) is therefore completely determined. In order to get a consistent picture of the optical properties of the carriers for high and low temperatures one proceeds as follows: One must first show that Eq. (10) gives a quantitative explanation of the frequency dependence of the optical absorption at low temperatures with the values of η and $\bar{\omega}$ determined from the high-temperature fit. One then determines the electronic-resonance integral J from a fit of the absolute magnitude of the optical effects. Finally, using (4) and (5), one has to show that this value for J is consistent with the high-temperature dc data that have been used for the fit of the high-temperature optical absorption and with the inequality (9). Note that the frequency dependence of $\text{Re}\sigma(\omega, \beta)$ in the high-temperature case, Eqs. (3) and (6), and in the high-frequency-low-temperature case, Eq. (10), has a simple structure. In particular, the frequency dependence in both cases is completely determined by the values of the two parameters η and $\bar{\omega}$. This simplicity is due to the fundamental assumption of sufficiently large dispersion of the optical phonons that has been made in the derivation of Eqs. (3), (6), and (10)

(see Refs. 1 and 2). The physical meaning and the importance of this assumption will become clear in the next subsection, where the general low-temperature expression for $\text{Re}\sigma(\omega, \beta \rightarrow \infty)$ is discussed.

C. The General Low-Temperature Case

Let us assume that phonons of r optical branches contribute to the building of the polarization around a localized small polaron. Denote by $\bar{\omega}_\nu$ the average frequency (first moment frequency) of the optical phonons in branch ν . Further, denote the spread of the phonon frequencies in branch ν around the average frequency by $\epsilon_d(\nu)\bar{\omega}_\nu$. Finally, η_ν is the average number of phonons of branch ν that contribute to the polaron formation. Again, η_ν is not necessarily an integer. Then from the definitions of η and of η_ν , it is seen that

$$\sum_{\nu=1}^r \eta_\nu = \eta. \quad (11)$$

Then $\text{Re}\sigma(\omega, \beta \rightarrow \infty)$ is given by

$$\text{Re}\sigma(\omega, \beta \rightarrow \infty) = 2^{3/2} J^2 a^2 e^2 N \pi \hbar^{-3} e^{-\eta} \times \sum_{n=1}^{\infty} \sum_{m_1 \dots m_r} \frac{\prod_{\nu=1}^r \eta_\nu^{m_\nu}}{\prod_{\nu=1}^r (m_\nu)! \sum_{\nu=1}^r m_\nu \bar{\omega}_\nu} g(\omega; m_\nu). \quad (12)$$

Here the sum over $m_1 \dots m_r$ is restricted to phonon combinations satisfying

$$\sum_{\nu=1}^r m_\nu = n, \quad (13)$$

and n is the order of the phonon sum process. The function $g(\omega; m_\nu)$ is a normalized Gaussian

$$g(\omega; m_\nu) = \exp\left[-\frac{1}{2}(\omega - \sum_{\nu=1}^r m_\nu \bar{\omega}_\nu)^2 / \Delta^2(m_\nu)\right] \times (2\pi)^{1/2} \Delta(m_\nu), \quad (14)$$

$$\Delta^2(m_\nu) = \frac{1}{4} \sum_{\nu=1}^r m_\nu \bar{\omega}_\nu^2 \epsilon_d(\nu). \quad (15)$$

The position of the maximum and the width of the Gaussian are both determined by the particular phonon sum combination characterized by a particular set of integers $m_1 \dots m_r$. The number of parameters has increased because each branch ν is now characterized by three parameters η_ν , $\bar{\omega}_\nu$, and $\epsilon_d(\nu)$. It is seen from (12) and (15) that for low frequencies the optical absorption is due to low-order phonon sum combinations. With increasing frequency the order n of the phonon sum processes is also increased. For light frequencies ω for which the main contribution is due to orders $n \leq 3$, considerable structure in the optical absorption is expected.

We are now in a position to discuss in detail the assumption of sufficiently large dispersion of the optical phonons and the physical implications of this assumption. Suppose that the average frequencies $\bar{\omega}_\nu$ of the r branches involved in polaron formation are not too close. Suppose further that the spread of allowed frequencies in each of the different branches is not too small. Then for light frequencies above a certain limit, phonon sum combinations of different orders n will contribute to the optical absorption because of the overlap in frequency of these different orders. The value of this low-limit light frequency is determined by the dispersion properties of the optical branches. Roughly speaking, the value of the limit frequency is the lower the higher the total dispersion of the r phonon branches under consideration. For light frequencies above the limit, the simultaneous contribution of different orders of the absorption leads to a gradual disappearance of structures due to any individual combination $m_1 \dots m_r$, because of the other possibilities with different sets of numbers. In other words, one gets a good continuum of endstates for the optical absorption due to multiphonon processes of different orders. This is exactly the situation described by Eq. (10) of the preceding subsection. Under condition (11), Eq. (12) must therefore lead to the same frequency dependence as Eq. (10) for frequencies above a certain limit, whose value is determined by the total dispersion in the r branches (and the distribution of η_ν over the different branches under study).

The situation described above is a consequence of the limit theorem for the distribution of sums of random variables. We shall come back to the frequency dependence of Eqs. (10) and (12) under the condition (11) in Sec. V in connection with the experimental results.

III. EXPERIMENTAL

Samples of about $7 \times 15 \times 1$ mm³ in size have been cut from crystals⁴ and optically polished. After the data on the bulk reflectivity had been taken, the samples were further lapped and optically polished down to thicknesses between 40 and 8.5 μ in order to permit transmission experiments.

The reflection and transmission spectra have been measured with a Grubb-Parson S3 spectrometer equipped with NaCl and KBr prisms. The instrument had been calibrated by recording the spectra of gases which have been measured with considerable accuracy on grating instruments.⁵

For the experiments at low temperatures a metal Dewar cell was used, which had been designed for both reflectivity and transmission measurements. Because of the small thicknesses of the samples used in the transmission experiments, the specimen was immersed in a He-gas atmosphere which provided the

⁴ P. Gerthsen, Z. Angew. Physik **15**, 301 (1963).

⁵ A. R. Downie, M. C. Magoon, T. Purcell, and B. Crawford, J. Opt. Soc. Am. **43**, 941 (1953).

thermal contact with the cooling liquid within a temperature difference less than 1°K. A more detailed description of the experimental techniques is given in Ref. 6.

From the reflection and transmission spectra, the values of the index of refraction n and the absorption coefficient K have been obtained by means of the following formulas:

$$n = \frac{1+R}{1-R} + \left[\frac{(1+R)^2}{(1-R)^2} - (1+k^2) \right]^{1/2}, \quad (16)$$

$$k = (1/4\pi)K\lambda, \quad (17)$$

$$K = d^{-1}[\sinh^{-1}(1-R)^2/2RT + \ln R], \quad (18)$$

where R is the reflectivity, T is the transmission, and d is the sample thickness. Equation (18) includes the

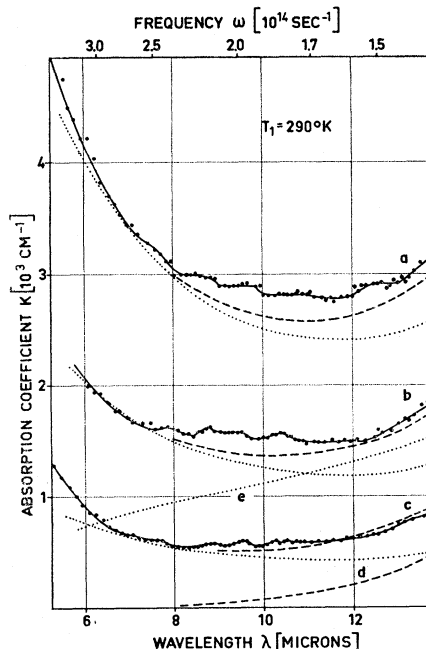


FIG. 2. Absorption coefficient of p -type LaCoO_3 for different dopants, $T_1 = 290^\circ\text{K}$. Full curves a-c: experimental data; dotted curves a-c: theoretical values for $K_{\text{carr}}(\omega)$ according to Eqs. (2)–(8); dashed curves coincide with dotted curves for $\lambda < 9$ microns. (a) $\sigma(0) = 12[\Omega \text{ cm}]^{-1}$, Sr dopant: 1 mole %; (b) $\sigma(0) = 6.5[\Omega \text{ cm}]^{-1}$, Sr dopant: 0.5 mole %; (c) $\sigma(0) = 2.2[\Omega \text{ cm}]^{-1}$, Sr dopant: 0.2 mole %; (d) $K_{\text{latt}}(\omega)$; (e) $K_{\text{carr}}(\text{Drude})(\omega)$; $\sigma(0) = 12[\Omega \text{ cm}]^{-1}$, $\tau_D = 3 \times 10^{-15}$ sec.

effect of multiple reflection but neglects interference effects which could be avoided for the most part by keeping the condition $Kd \gg 1$. The reflection and absorption spectra used as entries in Eqs. (16)–(18) are given in Ref. 6 and will not be reproduced here. The results for the absorption spectra are given in Sec. IV. For all the data taken the following inequality holds:

$$n^2 - k^2 \gg 2nk. \quad (19)$$

⁶ R. Mühlstroh, dissertation, Technische Hochschule Braunschweig, Braunschweig, Germany, 1967 (unpublished).

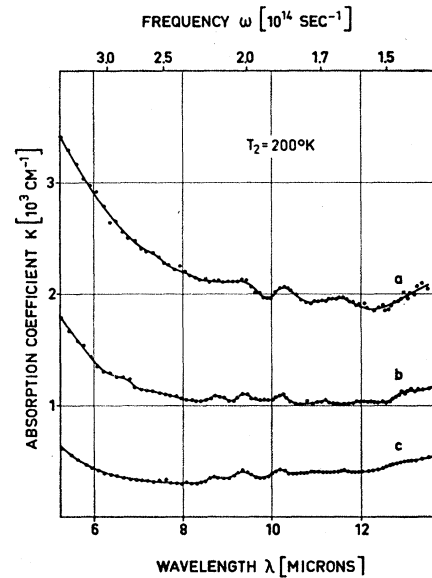


FIG. 3. Absorption coefficient of p -type LaCoO_3 for different dopants, $T_2 = 200^\circ\text{K}$. (For the dopant concentrations for curves a-c, see Fig. 2.)

This implies that for the analysis of the absorption spectra the simple relation (2) can be used.

IV. RESULTS

The optical data have been obtained for wavelengths between 14 and 3 μ which correspond to orders n between 2 and 10 for the different possible sum combinations to be described below. Figure 2 gives the absorp-

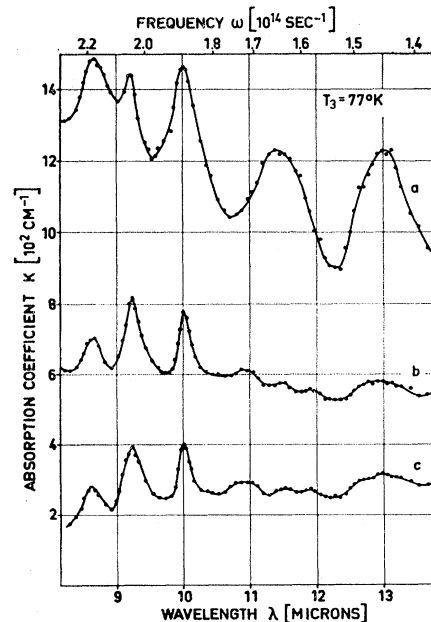


FIG. 4. Absorption coefficient of p -type LaCoO_3 in the range $8 < \lambda < 14 \mu$ for different dopants, $T_3 = 77^\circ\text{K}$. (For the dopant concentrations for curves a-c, see Fig. 2.)

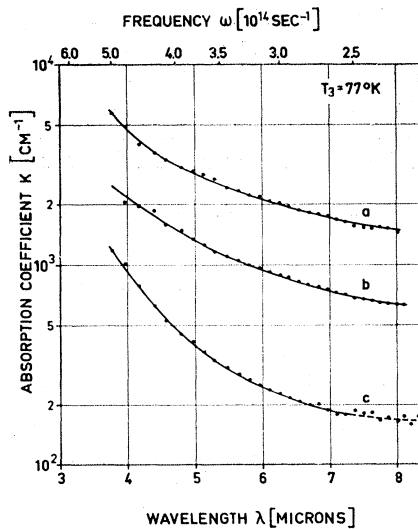


FIG. 5. Absorption coefficient of *p*-type LaCoO_3 in the range $3 < \lambda < 8 \mu$ for different dopants, $T_3 = 77^\circ\text{K}$. (For the dopant concentrations for curves a-c, see Fig. 2.)

tion coefficient K as a function of the wavelength for $T_1 = 290^\circ\text{K}$ and three samples of *p*-type LaCoO_3 with different dopants. For each frequency the relation between K and the dopant concentration N is linear. The extrapolation of this linear relation to $N \rightarrow 0$ gives the lattice contribution to the optical absorption $K_{\text{latt}}(\omega, \beta)$ (Fig. 2, curve d).⁷ The absolute magnitude of $K(\omega, \beta)$, as well as the frequency dependence, is strikingly different from that expected for a Drude-Zener gas of free electrons. The Drude-Zener behavior for a dopant corresponding to curve a is given in curve e. We can, therefore, from the start, exclude a free-carrier optical absorption of the well-known type. The optical

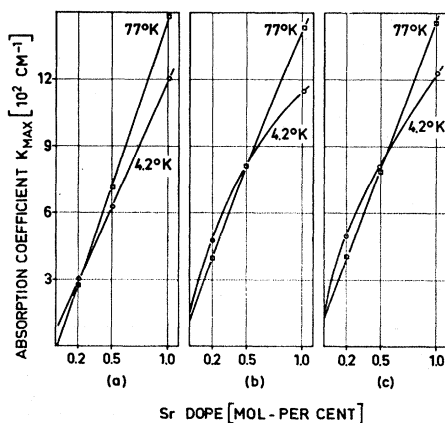


FIG. 6. Absorption coefficient versus Sr dope (mole %) for absorption peaks at the following wavelengths: (a) 8.6μ , (b) 9.2μ , (c) 9.9μ , corresponding to Figs. 4 and 7.

⁷ This rather unusual procedure had to be used because the stoichiometric samples did give nonreproducible absorption spectra because of native imperfections. This behavior of the stoichiometric and nearly stoichiometric samples also dictates the high dopant concentrations used in our experiments.

absorption has a minimum at 11μ . No structure is seen in the frequency dependence except for some small indications occurring between 8 and 11μ .

The optical absorption at $T_2 = 200^\circ\text{K}$ is given in Fig. 3 for the same samples. As is expected from the small-polaron theory, the absorption has decreased and the aforementioned structures between 8 and 11μ are more pronounced. The relation between $K(\omega, \beta)$ and the dopant concentration is still a linear one.

The optical absorption at $T_3 = 77^\circ\text{K}$ is given in Figs. 4 and 5 for the same samples. The absorption is further decreased, and considerable structure in the absorption is found between 8 and 13μ , whereas no structure could be detected for shorter wavelengths. The apparent

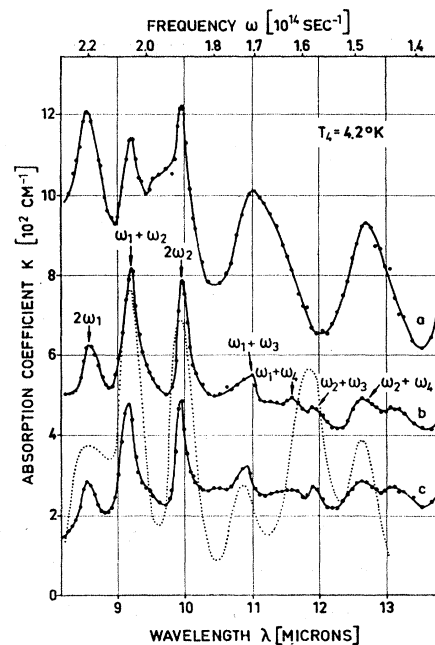


FIG. 7. Absorption coefficient of *p*-type LaCoO_3 in the range $8 < \lambda < 14 \mu$ for different dopants, $T_4 = 4.2^\circ\text{K}$. Full curves: experimental data. (For the dopant concentrations for curves a-c, see Fig. 2.) Dotted curve: theoretical values for $K_{\text{carr}}(\omega)$ according to Eqs. (11)–(15) fitted for a Sr dopant of 0.5 mole %.

structures in curve c of Fig. 5 between 7 and 8μ are from residual interference effects. The relation between $K(\omega, \beta)$ and the dopant concentration is still a linear one as shown by Figs. 6(a)–6(c) for the wavelengths 8.6 , 9.2 , and 9.9μ which correspond to the positions of the three most important absorption peaks in Fig. 4.

The optical absorption at $T_4 = 4.2^\circ\text{K}$ is shown in Figs. 7 and 8 for the same samples. The absorption pattern in general has not changed very much in between 77 and 4°K . A bit of the thermal background at 77°K has disappeared and the structures have further sharpened. The relation between $K(\omega, \beta \rightarrow \infty)$ and the dopant concentration N is no longer a linear one as shown by Figs. 6(a)–6(c). The absolute magnitude of the absorption coefficient between 8 and 14μ is much larger than the lattice absorption which is of the order

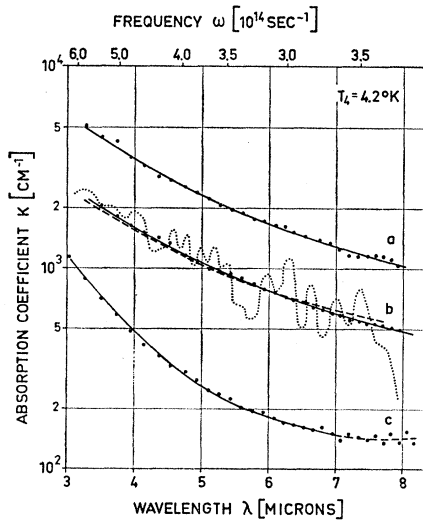


FIG. 8. Absorption coefficient of *p*-type LaCoO_3 in the range $3 < \lambda < 8 \mu$ for different dopants, $T_4 = 4.2^\circ\text{K}$. Full curves: experimental data. (For the dopant concentrations for curves a-c, see Fig. 2.) Dotted curve: theoretical values for $K_{\text{carr}}(\omega)$ according to Eqs. (11)–(15). Dashed curve: theoretical values for $K_{\text{carr}}(\omega)$ according to Eq. (10). Theoretical curves are fitted for an Sr dopant of 0.5 mole %.

$K_{\text{latt}} \approx 10^2 \text{ cm}^{-1}$. The absorption coefficient K increases with decreasing wavelengths between 8 and 3μ , in contradistinction to the behavior of the lattice absorption.

The absorption peaks between 8 and 13μ have nothing to do with the dopant atoms. This is shown by Fig. 9, where the absorption coefficient for *n*-type LaCoO_3 doped with Th is presented for T_1 and T_4 . The absorption peaks at T_4 are found at exactly the same positions as in *p*-type material doped with Sr. Localized modes can therefore be excluded.

V. ANALYSIS OF THE ABSORPTION SPECTRA

A. High-Temperature Case $T_1 = 290^\circ\text{K}$

The carrier contribution to the optical absorption has been calculated using Eqs. (2), (3), (6)–(8) with the experimental values for the index of refraction n and the dc conductivity $\sigma(\omega=0; \beta)$ for the values of the parameters $\eta = 9.2$ and $\bar{\omega} = 1.18 \times 10^{14} \text{ sec}^{-1}$. The average frequency $\bar{\omega}$ corresponds to $\bar{\lambda} = 16 \mu$ and is therefore consistent with the position of the reststrahlen band given in Fig. 1. Furthermore, using η and $\bar{\omega}$ one gets from (8) $\tau = 2.88 \times 10^{-15} \text{ sec}$ and therefore $\bar{\omega}\tau = 0.34$. The theoretical values for $K_{\text{carr}}(\omega, \beta)$ are given as dotted curves in Fig. 2. If the values of $K_{\text{latt}}(\omega, \beta)$ (curve e, Fig. 2) and $K_{\text{carr}}(\omega, \beta)$ are added, the dashed curves are obtained which are in good agreement with the experimental data.

In two short papers^{8,9} an analysis of the reflectivity

⁸ H. G. Reik, E. Kauer, and P. Gerthsen, Phys. Letters 8, 29 (1964).

⁹ H. G. Reik and R. Mühlstroh, Solid State Commun. 5, 105 (1967).

and absorption spectra have been given using the same theory with $\tau = 2.68 \times 10^{-15} \text{ sec}$, where, however, $\bar{\omega}\tau$ has been put equal to zero for simplicity. Comparison of Figs. 2 and 1 of Ref. 9 shows that a better agreement between theory and experiment is obtained for the realistic finite value of $\bar{\omega}\tau$ used in this paper.

B. Low-Temperature Case $T_4 = 4.2^\circ\text{K}$

Let us first turn to wavelengths between 8 and 3μ , where no structure is seen in the optical absorption. In this range no lattice absorption is expected and Eqs. (2) and (10) can be directly compared with the experimental values of $K(\omega, \beta \rightarrow \infty)$. For the analysis the experimental data for the index of refraction, the lattice constant $a = 3.82 \cdot 10^{-8} \text{ cm}$, and the dopant concentration for the 0.5% sample, $\text{Na}^3 = 0.5 \times 10^{-2}$, are used. Then, for the following values of the parameters of the theory $\eta = 9$, $\bar{\omega} = 1.18 \cdot 10^{14} \text{ sec}^{-1}$ and $J = 0.215 \text{ eV}$ the dashed curve in Fig. 8 is obtained, which is in excellent agreement with the experiments.

Let us turn next to wavelengths in between 8 and 14μ (see Fig. 7). It has already been mentioned that the structures in the absorption cannot be due to localized modes. The absorption peaks at the wavelengths 8.6, 9.2, 9.9, 10.9, 11.5, 11.9, and 12.7μ can, however, be explained as two-phonon sum combinations of four frequency bands in the one-phonon spectrum. The frequencies $\bar{\omega}_\nu$ ($\nu = 1, \dots, 4$) correspond to the wavelengths $\lambda_1 = 17.2 \mu$, $\lambda_2 = 19.9 \mu$, $\lambda_3 = 29.4 \mu$, $\lambda_4 = 34.5 \mu$. The assignment of phonon sum combinations to absorption peaks is indicated in Fig. 7. From the position of the

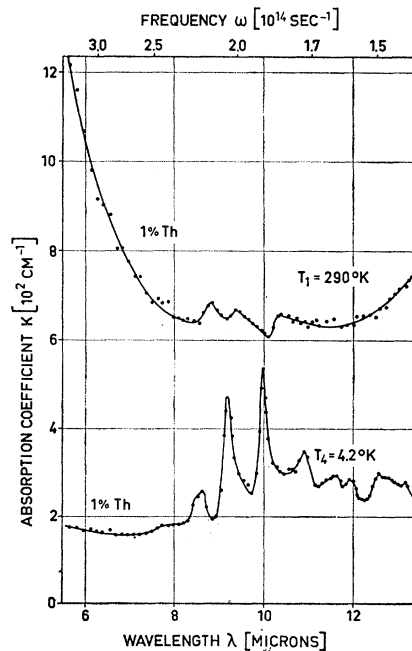


FIG. 9. Absorption coefficient of *n*-type LaCoO_3 with a Th dopant of 1 mole % at temperatures T_1 and T_4 .

reststrahlen band (Fig. 1), it seems plausible to attribute $\tilde{\omega}_1$ and $\tilde{\omega}_2$ to critical points in the longitudinal and in the transverse branch of this reststrahlen band. An assignment of $\tilde{\omega}_3$ and $\tilde{\omega}_4$ is not possible because nothing is known about the position of the other reststrahlen bands at lower frequencies.

The foregoing discussion shows that the low-temperature formulas (12)–(15) are applicable in principle because it is just the optical absorption accompanied by the emission of phonon sum combinations that they describe. However, from the practical point of view, an analysis of the data in this range of wavelengths meets with great difficulties. First of all, it is clear that the lattice contribution to the optical absorption $K_{\text{latt}}(\omega, \beta \rightarrow \infty)$ is not negligible. However, apart from the order of magnitude, nothing is known of the lattice contribution. Again, the stoichiometric samples give an irreproducible optical absorption (see Ref. 7). Furthermore, the extrapolation procedure for obtaining $K_{\text{latt}}(\omega, \beta)$ described in Sec. 4 for the high-temperature experiments is no longer applicable because the relation between the optical absorption and the dopant concentration is not linear at helium temperatures (see Fig. 6). Further difficulties arise with the evaluation of the carrier contribution $K_{\text{car}}(\omega, \beta \rightarrow \infty)$. With our experimental equipment we can only detect the coupling between the polaron and those branches of the optical-phonon spectrum whose two-phonon sum combinations make their appearance in the range of wavelengths between 8 and 14 μ , which are just the ones discussed above. It is therefore to be suspected that the information put into Eqs. (12)–(15) is incomplete and that an analysis of the optical data based on it is of a highly qualitative nature.

This is clearly shown by the dotted curve in Figs. 7 and 8, which has been obtained from Eq. (2), (12)–(15) with the values of $\tilde{\omega}_\nu$ given before, $\epsilon_d(\nu) = 0.05$ for all branches, $\eta_1 = 3.0$, $\eta_2 = 5.0$, $\eta_3 = 1.25$, $\eta_4 = 0.75$, and $J = 0.174$ eV. As is seen, $\sum_{\nu=1}^4 \eta_\nu = \eta = 10$, which is close to the value $\eta = 9$ used before. In the wavelength range between 8 and 14 μ the dotted curve describes the qualitative features of the experiments. The deviations between theory and experiment are of the order of magnitude of the lattice contribution.

For smaller wavelengths (see Fig. 8), the dotted curve has too much structure, although on the average it gives the right frequency dependence, in particular at small wavelengths. After having described the frequency dependence of the optical absorption given by the dotted curve, let us now proceed to discuss it. Let us assume for this purpose that we had available all the exact information needed for the evaluation of Eqs. (2), (12)–(15), and in particular that $\sum_{\nu=1}^r \eta_\nu = 10$.

Looking at the dotted curve from this point of view, we would say that we had purposely overestimated the contribution of some of the branches and purposely

neglected the contribution of others under the condition of constant η . It is now immediately obvious that the dotted curve must give too little background in Fig. 7 and too much structure in Fig. 8. For all frequencies where absorption takes place by combinations of $\omega_1, \dots, \omega_4$, one overestimates the absorption and consequently underestimates the absorption at other places. The fact that the structures of the dotted curves gradually disappear with shorter wavelengths is due to the properties of the distributions of sums of random variables, mentioned at the end of Sec. II. The limit theorem applied to the present case says that the influence of the details of the one-phonon dispersion on the frequency dependence of the optical absorption decreases with increasing light frequency, that is, with increasing order of the phonon sum processes. In other words, for sufficiently high frequencies the values of $\tilde{\omega}_\nu$, $\epsilon_d(\nu)$, η_ν are no longer needed. The two average parameters η and $\tilde{\omega}$ are sufficient to characterize the frequency dependence of the optical absorption at high frequencies. The fact that the dotted curve on the average gives the right frequency dependence of the optical absorption for short wavelengths shows that the values of η_ν given above are consistent with the value $\eta = 9$ used in the evaluation of Eq. (10) which applies in the high-frequency limit. The results of the analysis are also consistent with the dc data. Using $\eta = 9$, $\tilde{\omega} = 1.18 \times 10^{14}$ sec⁻¹, and $\mu = 2.8 \times 10^{-1}$ cm²/V sec,¹⁰ we obtain from Eq. (5) $J = 0.224$ eV, in excellent agreement with the values taken from the optical data. The condition of the applicability of the theory, the inequality (9), is satisfied.

VI. CONCLUSION

The results of Secs. IV and V show that a consistent interpretation of the optical properties of semiconducting LaCoO₃ at high and low temperatures is possible in terms of the small-polaron picture. One gets quantitative agreement between theory and experiment for high temperatures.

For low temperatures a quantitative agreement between theory and experiment is found for wavelengths between 3 and 8 μ . For $\lambda > 8 \mu$ the agreement is only qualitative because of our incomplete knowledge of the lattice properties. The values of the parameters of the theory used for the fit of the optical data at high and low temperatures are consistent with each other.

ACKNOWLEDGMENTS

The authors thank Professor D. Polder (Eindhoven) for helpful and stimulating discussions and Dr. K. H. Hardtl (Aachen) for providing the crystals.

¹⁰ P. Gerthsen and K. H. Hardtl, Z. Naturforsch. 17a, 514 (1962).